



Gas-particle partitioning of pesticides in the atmosphere of the North China Plain

Liping Guo¹, Shuping Shi¹, Ying Li², Martin Brüggemann³, Mingyu Zhao¹, Hongyu Mu¹,

Daniel M. Figueiredo⁴, Junxue Wu⁵, Kai Wang¹ *

¹ State Key Laboratory of Nutrient Use and Management, College of Resources and Environmental Sciences; National Academy of Agriculture Green Development; Key Laboratory of Plant-Soil Interactions of Ministry of Education, National Observation and Research Station of Agriculture Green Development (Quzhou, Hebei), China Agricultural University, Beijing 100193, PR China, ² Key Laboratory of Industrial Ecology and Environmental Engineering (Ministry of Education), School of Environmental Science and Technology, Dalian University of Technology, Dalian 116024, China, ³ Bayer AG, Crop Science Division, R&D, Environmental Safety, Monheim, Germany, ⁴ Institute for Risk Assessment Sciences, Utrecht University, 3584 CM Utrecht, Netherlands, ⁵ Institute of Plant Protection, Beijing Academy of Agriculture and Forestry Science, Beijing 100097, China

Corresponding Author: Kai Wang, Email: kaiwang_ly@cau.edu.cn



1 **Abstract:** Pesticide residues are ubiquitous in the atmosphere in the North China Plain (NCP),
2 with concentrations largely determined by application patterns and physicochemical parameters
3 such as persistence and volatility. However, knowledge of gas-particle partitioning of pesticides
4 remains limited, hindering a comprehensive understanding of their abundance, transport, and
5 health risks. Here, we aim to elucidate the underlying mechanism of gas-particle partitioning
6 for pesticides. In this study, 14 pairs of air and particulate matter samples were collected
7 simultaneously in Quzhou County, the NCP. A total of 19 pesticides were observed in both gas
8 and particulate-phases. Average pesticide concentrations in particulate phase ($2025.76 \pm$
9 1048.83 pg/m^3) were significantly higher than in gas phase ($143.38 \pm 146.31 \text{ pg/m}^3$),
10 accounting for 93.4% of the total atmospheric pesticide mass. Tebuconazole (662.49 ± 448.52
11 pg/m^3), pyraclostrobin ($212.01 \pm 119.70 \text{ pg/m}^3$), and carbendazim ($158.68 \pm 86.54 \text{ pg/m}^3$)
12 exhibited the highest concentrations in the particulate phase, whereas pyrimethanil ($93.00 \pm$
13 79.18 pg/m^3), pymetrozine ($22.96 \pm 21.50 \text{ pg/m}^3$), and imidacloprid ($5.78 \pm 2.64 \text{ pg/m}^3$)
14 were predominant in the gas phase. A positive correlation between temperature and particulate-
15 phase pesticide concentrations was found, as indicated by rising of $\log K_p$ values which is likely
16 attributable to an interplay of pesticide physicochemical properties, ambient relative humidity,
17 particle phase state and pesticide use patterns. Gas-particle partitioning model simulations
18 showed absorption as the main mechanism of gas-particle partitioning, indicating atmospheric
19 pesticides are absorbed into the interior organic film of particulate matter.

20
21 **Keywords:** Atmospheric pesticide, Gas-particle partitioning, Influence factor, the North
22 China Plain

23

24

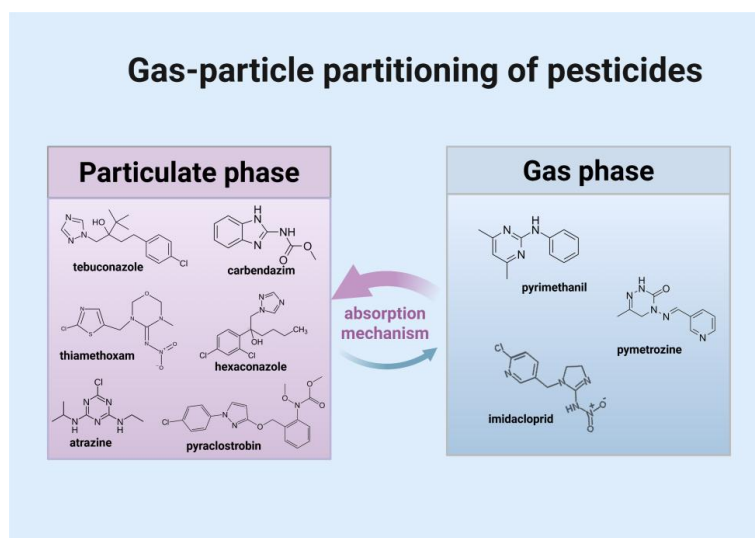
25

26

27



28 Graphic Abstract:



29
 30
 31
 32
 33

1 Introduction

34 Pesticides have been widely applied worldwide against pests in agriculture since
 35 dichlorodiphenyltrichloroethane (DDT) was discovered to have insecticidal properties in 1939
 36 (Turusov et al., 2002). Pesticides play an important role in the development of agriculture by
 37 increasing the yield of agricultural products and improving their quality (Aktar et al., 2009).
 38 Pesticide usage in China reached 229,026 metric tons in 2023, accounting for around 6.14% of
 39 global pesticide use (FAO, 2025). However, the pesticide utilization rate (the proportion of the
 40 pesticide deposited on the target per unit area to the total amount of pesticide used) for the three
 41 major cereal crops (i.e., wheat, maize and rice) in China was only about 41% (China, 2021)
 42 meaning that more than half of the pesticides were not effectively absorbed by the target crops
 43 or pests and was instead lost to the environment (e.g., water, soil and atmosphere) (Tudi et al.,
 44 2022). While the fate of pesticides in soil and water has been studied extensively over the last



45 decades, their behavior, distribution, and degradation in the atmosphere have only recently
46 gained increasing interest (Brüggemann et al., 2024). There are mainly three ways for pesticides
47 to enter the atmosphere: drift, volatilization, and wind erosion. In detail this means that a portion
48 of applied pesticides reaches the atmosphere directly during application (e.g. spray drift and
49 vapor drift) (van den Berg et al., 1999). Later, after application, soil particles that have adsorbed
50 pesticides may serve as a reservoir and release residues into the atmosphere through
51 resuspension of soil particles, also referred to as wind erosion (Glotfelty et al., 1989).
52 Furthermore, pesticides may volatilize from plants, soil, surface water, and the surfaces of old
53 industrial sites under the influence of diffusive air-surface mass exchange (Cabrerizo et al.,
54 2011).

55 Upon entering the air, gas-particle partitioning occurs between the gas phase and particulate
56 phase depending on the physicochemical properties of the pesticides (e.g., vapor pressure,
57 octanol-air partition coefficient, K_{oa}), the concentrations of total suspended particulate matter
58 (TSP) and meteorological parameters (ambient temperature and relative humidity). Among
59 these factors, vapor pressure (V_P) is widely acknowledged as the main factor determining the
60 effective volatilization rates. Pesticides with V_P (at 20 °C) higher than 1×10^{-2} Pa are
61 predominantly present in the gas phase, while those with V_P below 1×10^{-5} Pa can be seen as
62 completely present in the particulate phase (Yusà et al., 2009). The conventional Junge-Pankow
63 model attributes particle/gas partitioning to surface adsorption, whereas the absorption model
64 assumes that chemicals dissolve into particles coated by organic films (Harner and Bidleman,
65 1998). Since most pesticides are semi-volatile compounds with moderate vapor pressure, they
66 are distributed in both the gas phase and particulate phase (Bedos et al., 2002; Wang et al.,



2024). Pesticides in the gas phase can be directly absorbed into the lungs and participate in the blood circulation, potentially causing adverse effects on the cardiovascular system and almost all organs (Ngo et al., 2010). The pesticides in fine particulate matter are able to penetrate deeply into the respiratory system, causing a spectrum of health hazards (Woodrow et al., 2019). These pesticides have the potential to affect various systems, such as the respiratory, circulatory, immune, and endocrine systems, and may even contribute to carcinogenesis (Kaur et al., 2019). A previous study demonstrated that the half-lives in particulate phase of difenoconazole, tetraconazole, fipronil and 8 other pesticides were longer than the estimated half-lives in the gas phase allowing them to travel longer distances (Socorro et al., 2016). Because of the different behavior and effects of gas-phase and particulate-phase pesticides on human health and the environment, it is of great significance to study the gas-particle partitioning of atmospheric pesticides for further analysis of their health and ecotoxicological effects (Brüggemann et al., 2024).

In recent years, studies on the gas-particle partitioning of pesticides in the atmosphere mainly focused on traditional pesticides, such as organochlorine pesticides (Qiao et al., 2019). Sanli et al. studied the partitioning of organochlorine pesticides in gas phase and particulate phase at a semi-rural site in Bursa, Turkey, suggesting that the maximum annual mean gas-phase organochlorine pesticides concentration was β -hexachlorocyclohexane (β -HCH) with 176 pg/m^3 while the maximum concentration in the particulate phase was β -Endosulfan at 67 pg/m^3 (Sanlı and Tasdemir, 2020). However, due to their long lifetime in the environment, most of these pesticides are now prohibited in most countries. In contrast, modern substances exhibit significantly shorter degradation times in the environment. Still, data on gas-particle



89 partitioning of such current-use pesticides are rarely available. Wang et al. measured the
90 atmospheric concentrations of 36 current-use pesticides in gas phase and particulate phase
91 samples in the Great Lakes basin and analyzed their gas-particle partitioning, suggesting that
92 chemicals in particulate phase like metolachlor were negatively correlated with relative
93 humidity (Wang et al., 2021). Nevertheless, there is limited evidence on the mechanism of
94 pesticides gas-particle partitioning, which hinders our understanding of the atmospheric fate,
95 transport and health risks of pesticides. Therefore, it is necessary to further research and
96 understand the gas-particle partitioning of pesticides in the atmosphere.

97 Quzhou County is located in the center of the North China Plain (NCP), which is the region
98 with the highest degree of intensive farming in China. As a typical agricultural county in the
99 NCP situated in the northeast of Handan City, Hebei Province, at geographical coordinates of
100 $36^{\circ}35'43''$ - $36^{\circ}57'56''$ N, $114^{\circ}50'22''$ - $115^{\circ}13'27''$ E (Yu et al., 2021), Quzhou serves as an ideal
101 location for investigating gas-particle partitioning of atmospheric pesticides, facilitating a more
102 comprehensive understanding of pesticide distribution within the NCP (Feng et al., 2022). This
103 study attempts to (1) analyze the concentrations of atmospheric pesticides in both gas and
104 particulate phases; (2) assess the effect of meteorological factors on pesticide concentrations in
105 the atmosphere, and (3) investigate gas-particle partitioning mechanisms using three different
106 partitioning prediction models.

107 **2 Materials and Methods**

108 **2.1 Air sampling**

109 A high-volume air sampler (Sibata Scientific Technology Ltd, 080130-1203) fitted with a
110 polyurethane foam plug (PUF, 90 mm in diameter \times 50 mm in thickness) and a quartz fiber



111 filter (QFF, 203 mm × 254 mm, pore size <0.3 μm) was used to capture pesticides in the gas
112 phase and particulate phase (i.e. TSP), respectively. Air samples were collected with a sampling
113 period of 7 days (168 hours) at a flow rate of 150 L min⁻¹ from February 17th to May 20th in
114 2023 at the Quzhou Experiment Station (36°78'01"N, 114°94'51"E, 40 m above sea level) in
115 Quzhou County, the NCP. Detailed sampling information is provided in Table S1. In total, 14
116 gas phase samples and 14 particulate phase samples were collected. All samples were kept at –
117 20°C until analysis. Meteorological data (Table S2), including temperature, atmospheric
118 pressure, precipitation, relative humidity, and wind speed, along with particulate matter (PM₁₀
119 and PM_{2.5}) concentrations, were obtained from the Air Quality Monitoring Platform of Handan
120 City (<http://111.62.17.169:8083/index.html#/map/HomeTianMap>) and the Quzhou
121 Experimental Station. The mass of TSP was measured by gravimetry.

122 **2.2 Sample treatment and instrumental analysis**

123 The PUFs and QFFs were extracted with ultrasound-assisted extraction for 1 hour with a 100
124 mL mixture of hexane and dichloromethane (1:1, v-v). The extracts (80 mL) were collected in
125 flat-bottomed flasks and then concentrated to dryness using a rotary evaporator. Next, 1 mL
126 acetonitrile was added to each flat-bottomed flask and transferred to the centrifuge tube after
127 sonication, with this process repeated twice. After concentration, the extracts were subsequently
128 purified on C₁₈ SPE cartridges and the columns were eluted with 5 mL of acetonitrile. All
129 fractions were rotary evaporated to dryness and adjusted to a volume of 800 μL with acetonitrile.
130 Finally, they were vortexed using a vortex oscillator and filtered with syringe filters and
131 transferred to vials for detection.



132 Target analytes in this study included 17 fungicides, 4 herbicides, and 17 insecticides for a total
133 of 38 compounds purchased from Alta Scientific Co., Ltd (Tianjin, China) (Table S3). All
134 solvents and chemicals used in this study were of high-performance liquid chromatography
135 (HPLC) grade or higher. A Waters ACQUITY TQD ultra-high performance liquid
136 chromatography system coupled with a triple-quadrupole mass spectrometer (UHPLC-MS/MS)
137 was used to analyze the pesticides. The chromatographic and mass spectrometric conditions
138 were consistent with Zhao et al. (Zhao et al., 2023). The UHPLC-MS/MS equipped with an
139 ACQUITY BEH C18 column (1.7 μm , 100 \times 2.1 mm i.d.). The mobile phase is increased
140 from 5% acetonitrile (A) and 95% ultra-pure water with 0.1% formic acid (B) at 0 minutes to
141 95% acetonitrile over 6 minutes, then decreased to 5% A over 0.5 minutes and held for 0.5
142 minutes. The flow rate was 0.2 mL min⁻¹ and 2 μL of individual sample was injected. The
143 column temperature was set at 40°C. The mass spectrometer was operated in multiple reaction
144 monitoring (MRM) mode. The calculation method for pesticide mass concentration in ambient
145 air is provided in the Supporting Information (Text S1).

146 **2.3 Quality assurance and quality control**

147 To evaluate the accuracy and reliability of the data, laboratory blanks were analyzed following
148 the same procedure as the samples, and the measured concentrations of the laboratory blank
149 samples were very low, indicating minimal contamination during processing. The
150 reproducibility of the spiked blanks was acceptable, yielding recoveries ranging from 45.10%
151 \pm 3.36% to 105.3% \pm 3.29% for gas phase and 45.40% \pm 2.64% to 122.50% \pm 12.51% for
152 particulate phase. Except for etoxazole in the gas phase (45.1%) and cycloxyaprid and
153 thiophanate-methyl in the particulate phase (both 45.4%), most pesticides showed good



recovery extracted by dichloromethane and hexane. The average recoveries for 38 pesticides was $74.0 \pm 22.5\%$ in the particulate phase and $73.5 \pm 16.8\%$ in the gas phase. All concentration data of this study is not adjusted using the recoveries. The limit of detection (LOD) was estimated as the quantity of analyte with a signal to noise ratio of 3:1, ranging from 0.01 pg/m^3 to 9.32 pg/m^3 for gas phase samples and from $2.22 \times 10^{-4} \text{ pg/m}^3$ to 5.89 pg/m^3 for particulate phase samples (Table S4).

2.4 Gas-particle partitioning models

Partitioning of pesticides between the gas phase and particulate phase is often described using the gas-particle partitioning coefficient (K_p , $\text{m}^3/\mu\text{g}$) which defined by Harner and Bidleman (Harner and Bidleman, 1998):

$$K_p = \frac{C_p}{C_g \times C_{TSP}} \quad (1)$$

Where C_p and C_g are the concentrations of the pesticides ($\mu\text{g}/\text{m}^3$) in the particulate phase and gas phase, respectively and C_{TSP} is the concentration of the TSP in the air ($\mu\text{g}/\text{m}^3$).

The measured particle-bound fraction (ϕ_m) can be calculated by the equation(2):

$$\phi_m = \frac{C_p}{C_p + C_g} \quad (2)$$

The Junge-Pankow (J-P) adsorptive model assumes that the organic matter is adsorbed onto aerosol surface and relates the predicted particle-bound fraction (ϕ_p) to the aerosol surface area per air volume unit and the saturation vapor pressure of supercooled liquid (P_L^0 , Pa) values (Pankow, 1987). The ϕ_p can be calculated by the equation (3):

$$\phi_p = \frac{c\theta}{c\theta + P_L^0} \quad (3)$$



174 Where ϕ is the fraction of organic matter concentration that is adsorbed onto the aerosol surface.
 175 The parameter c is a constant with an empirical value of 17.2 Pa/cm. θ represents the
 176 contaminated aerosol surface area per unit air volume (cm^2/cm^3) with a series of representative
 177 values ($1.0 \times 10^{-7} \text{ cm}^2/\text{cm}^3$ for remote areas, $1.0 \times 10^{-6} \text{ cm}^2/\text{cm}^3$ for rural areas, and 1.1×10^{-5}
 178 cm^2/cm^3 for urban areas). P_L^0 is subcooled liquid vapor pressure calculated according to the
 179 MPBPVP module in the Estimation Program Interface (EPI) suite (EPIWEB-4.1) of the U.S.
 180 Environmental Protection Agency (U.S.EPA) using the mean temperature (K) during each
 181 sampling period, for the pesticides atrazine, carbendazim, difenoconazole, prochloraz,
 182 tebuconazole, hexaconazole, propiconazole, pyrimethanil, and omethoate, the P_L^0 values at
 183 25°C were used as substitutes, since values at the actual temperature were unavailable in this
 184 module (Lohmann et al., 2004). $\text{Log}P_L^0$ values for the studied pesticides are presented in Table
 185 S5.

186 The Harner-Bidleman (H-B) K_{oa} absorption model predicts K_p as a function of K_{oa} and the
 187 fraction of organic matter in the aerosols (f_{om}), assuming that the organic matter is absorbed
 188 into a liquid-like organic film in the particulate matter under the influence of the absorption
 189 force, solubility and particle size (Harner and Bidleman, 1998; He and Balasubramanian, 2009):

$$190 \quad \text{Log } K_p = \text{log } K_{oa} + \text{log } f_{om} - 11.91 \quad (4)$$

191 Where f_{om} is fraction of organic matter in the aerosols and four f_{om} values of 5%, 10%, 20%
 192 and 30% were introduced (Jiang et al., 2020). K_{oa} was calculated according to the method in
 193 KOAWIN module of the EPI suite of the U.S.EPA and the equation is as follows (Baskaran et
 194 al., 2021):



$$K_{oa} = \frac{K_{ow} \cdot RT}{HLC} \quad (5)$$

where the K_{ow} is the octanol-water partition coefficient, with the value at 25°C acquired from the KOWWIN module in the EPI suite (EPIWEB-4.1) of the U.S.EPA. $\log K_{oa}$ values for the studied pesticides are presented in Table S6. R is the ideal gas constant (Pa mol/K/m^3) with a value of 8.314. T is the mean temperature during each sampling period (K). HLC is Henry's law constant calculated according to the equation acquired from the HENRYWIN module in the EPI suite (EPIWEB-4.1) of the U.S. EPA:

$$\ln HLC = A_n - B_n/T \quad (6)$$

where T is the mean temperature (K) during each sampling period. The A_n and B_n of each pesticide are different and the specific values were obtained in the HENRYWIN module.

Additionally, the φ_p can be predicted by:

$$\varphi_p = 1 / \left\{ 1 + \left[\frac{1}{(10^{-11.9} \cdot f_{om} \cdot K_{oa}) \cdot TSP} \right] \right\} \quad (7)$$

The TSP values for each sampling period were used in this study and the typical values (5%, 10%, 20% and 30%) of f_{om} were also inserted.

The L-M-Y model was a steady-state model established by Li et al. in 2015, which considered the influences of dry and wet depositions of particles and introduced into a non-equilibrium parameter caused by dry and wet depositions, $\log \alpha$ (McEachran Andrew et al., 2015). And the $\log K_{P-L-M-Y}$ and φ_{L-M-Y} can be predicted according to the equations (8) and (9) as follows:

$$\log K_{P-L-M-Y} = \log K_{p-H-B} + \log \alpha \quad (8)$$

$$\varphi_{L-M-Y} = \frac{K_{p-H-B} \cdot \alpha \cdot TSP}{1 + K_{p-H-B} \cdot \alpha \cdot TSP} \quad (9)$$



215 The Log K_{P-H-B} can be calculated by equation (4) and the $\log \alpha$ can be calculated by

$$216 \quad \text{Log } \alpha = -\text{Log} \left[1 + \left(\frac{2.09 \times 10^{-10} f_{om} K_{oa}}{C} \right) \right] \quad (10)$$

217 The values of f_{om} and the empirical constant C relative to prevailing wind were cited from
 218 previous studies ($f_{om} = 5\%, 10\%, 20\%$ and 30% , $C = 5$) in the above model (Iakovides et al.,
 219 2022).

220 Calculation of root mean square errors (RMSE): RMSE for each φ_p of the pesticides detected
 221 in the gas phase and the particulate phase at the same time was calculated to statistically
 222 evaluate each partitioning model and the lower the RMSE value is, the closer is the φ_p to φ_m ,
 223 indicating that the model has a better prediction of the gas-particle partitioning of the pesticides
 224 in the studied area. The RMSE can be calculated according to the equation as follows:

$$225 \quad RMSE = \sqrt{\frac{\sum_{i=1}^n (\varphi_{mi} - \varphi_{pi})^2}{N}} \quad (11)$$

226 Where φ_{mi} is the measured particle fraction of each pesticide, φ_{pi} is the particle fraction predicted
 227 by each model, and N is the sample size.

228 **3 Results and discussion**

229 **3.1 Detection frequency of pesticides in ambient air**

230 A total of 33 pesticides was observed in the gas phase and particulate phase samples of Quzhou
 231 County during the sampling period from February 2023 to May 2023, including 17 fungicides,
 232 12 insecticides, and 4 herbicides. The detection frequencies of these pesticides varied from 7.14 %
 233 (thiacloprid) to 100 % (acetamiprid). The detection frequencies for all quantified pesticides are
 234 given in Table S7. Twenty individual pesticides were detected at least once in both gas and



particle-phase samples, with acetamiprid, imidacloprid, difenoconazole, pymetrozine, and tebuconazole detected in > 50% samples. Notably, fipronil, a pyrazole insecticide banned in agricultural production in China since 2009 (Ministry of Agriculture and Rural Affairs of the People's Republic of China, 2009), was detected in particulate phase samples on March 31st for the first time and continued to be detected in subsequent particulate phase samples until the end of sampling on May 20th, which might be due to the use of fipronil as sanitary or seed coating agent of partial dryland crop in the vicinity of the sampling site, as well as its application in controlling household pests (Cui et al., 2016).

Compared with the detection frequencies of pesticides in gas phase (64.29-85.71%), the detection frequencies in particulate phase were relatively high (71.43-92.86%). The pesticides of clothianidin, chlorobenzuron, dimethomorph, fipronil, propamocarb, thiophanate-methyl, tribenuron-methyl, triadimenol, kresoxim-methyl, azoxystrobin, trifloxystrobin and pyraclostrobin were detected only in the particulate phase.

3.2 Concentrations of pesticides in ambient air

In total 33 pesticides were observed with the applied UHPLC-MS/MS method, including 12 insecticides, 4 herbicides and 17 fungicides (Figure 1). The average concentrations of pesticide in particulate phase ($2025.76 \pm 1048.83 \text{ pg/m}^3$) were significantly higher than $143.38 \pm 146.31 \text{ pg/m}^3$ in gas phase), constituting 93.4% of the total atmospheric pesticide mass. In the particulate phase, the mean concentration of tebuconazole (a broad-spectrum triazole fungicide) in the 14 QFF samples was the highest with a value of 662.49 pg/m^3 , and the mean concentration of thiophanate-methyl (a thioureas fungicide) was the lowest with a value of



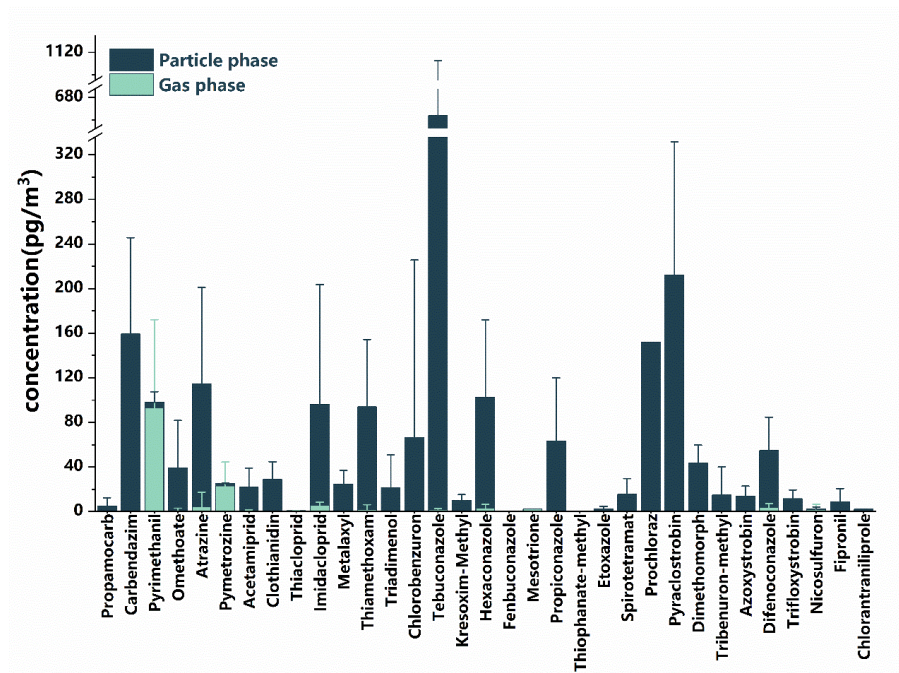
256 0.015 pg/m³. In the gas phase, pyrimethanil (an aminopyrimidines fungicide) shows the highest
257 average concentration (93.00 µg/m³) in the 14 PUF samples, attributed to its high vapor
258 pressure—second only to propamocarb—facilitating its volatilization, and the mean
259 concentration of fenbuconazole (a triazole fungicide) was the lowest with a value of 0.05 pg/m³.
260 Research has found that the pesticides in atmospheric aerosol particles are very persistent
261 because the particles shield the absorbed compounds from degradation by OH radicals (Socorro
262 et al., 2016). In addition, atrazine, omethoate and pyrimethanil were detected in samples taken
263 around April 14th and the samples taken later in the gas phase, probably owing to the
264 application or the fact that with the temperature raised, there was re-volatilization of this
265 pesticide from contaminated terrestrial surfaces (Gungormus et al., 2021). Moreover, the
266 pesticide physicochemical properties, their environmental persistence and the pesticide
267 application technique used may also influence the atmospheric concentrations of the pesticides
268 (Degrendele et al., 2016). Detailed average concentration for individual pesticides in the 14
269 gas-phase and 14 particulate-phase samples collected during the sampling period from February
270 2023 to May 2023 are given in Table S8.

271 Neonicotinoid insecticides (NEOs) stand as the most extensively applied pesticides across
272 agriculture, boasting versatile applications such as seed dressing, spraying, and soil application
273 (Zhou et al., 2020). The average concentration of NEOs including acetamiprid, clothianidin,
274 imidacloprid, thiamethoxam and thiacloprid in atmosphere was 241.18 pg/m³, while it was
275 232.03 pg/m³ for particulate phase and 9.15 pg/m³ for gas phase. This is at the same level as
276 the gaseous pesticides reported by Zhao et al. in Quzhou County, the NCP (0.6–26 pg/m³). In
277 comparison, the average concentration of NEOs in the particulate phase observed in this study



278 was substantially higher than that associated with PM_{2.5} in an urban area of Beijing, China
279 (35.8 pg/m³) and nearly three times greater than the PM_{2.5}-bound concentration reported for a
280 rural area of Zhengzhou City, China (80.9 pg/m³), a conventional agricultural region, as
281 reported by Zhou et al. (Zhou et al., 2020). Meanwhile, the concentration of individual NEOs
282 for particulate phase (90.42 pg/m³, 20.63 pg/m³, 91.82 pg/m³ and 28.71 pg/m³ for imidacloprid,
283 acetamiprid, thiamethoxam and clothianidin, respectively) was higher than that in the rural area
284 of Zhengzhou City, China (48.00 pg/m³, 17.70 pg/m³, 7.20 pg/m³ and 7.95 pg/m³, respectively),
285 probably due to that pesticides observed in our study were in the TSP samples (including
286 particles with all sizes), whereas the particulate samples in the rural areas of Zhengzhou City,
287 China were the PM_{2.5} fraction. A study by Hu et al. (Hu et al., 2024) on risk assessment of
288 airborne agricultural pesticide exposure near the field in the grain growing area in Liaocheng
289 City, China detected concentrations of acetaminiprid, atrazine, imidacloprid and nicosulfuron at
290 4.88×10^5 pg/m³, 2.17×10^3 pg/m³, 4.11×10^4 pg/m³, 3.46×10^4 pg/m³, respectively. The mean
291 concentration of the above pesticides in our study (21.66, 114.72, 96.19 and 2.17 pg/m³) was
292 lower than that of the research in Liaocheng City, China, which may be related to the low
293 pesticide application near the sampling site during the sampling period in this study.

294



295
296 Figure 1. The average concentration of individual pesticide in the 14 gas phase (light green)
297 and 14 particulate phase (dark green) samples collected during the sampling period from
298 February 2023 to May 2023. In total 33 pesticides were observed with the applied UHPLC-
299 MS/MS method.

300 **3.3 Temporal variation of pesticide concentration**

301 The concentrations of four typical fungicides (i.e., tebuconazole, prochloraz, pyraclostrobin,
302 and propiconazole) and the insecticide imidacloprid increased in the particulate phase in mid-
303 April and early May (Figure 2, Figures S1-S2). In the gas phase, imidacloprid, atrazine,
304 tebuconazole, and propiconazole showed a similar trend but at lower concentrations than in the
305 particulate phase, except for pyrimethanil, which had a higher concentration in the gas phase
306 on April 29th. The concentration of hexaconazole in the gas phase and the particulate phase had
307 a similar trend over time (Figures S1–S2). This trend aligns with the application timing during



the booting and heading stages of wheat, with peak concentrations coinciding with pesticide application. In addition, the concentrations of hexaconazole and imidacloprid in the gas phase were higher than particulate phase before April (the month of wheat booting stage), this might be caused by the evaporation of pesticides from the soil to the atmosphere. Although the temporal distribution patterns of other pesticides in the gas and particulate phases do not exhibit a high degree of consistency, the concentrations of most pesticides in the particulate phase increased to some extent between mid-April and May (Figures S1–S2). These findings suggest that pesticide applications near the sampling site resulted in emissions into the atmosphere and subsequent association with atmospheric particulate matter. Moreover, the temporal pattern indicates that local sources (e.g., pesticides application in the local fields) dominated atmospheric pesticide concentrations.

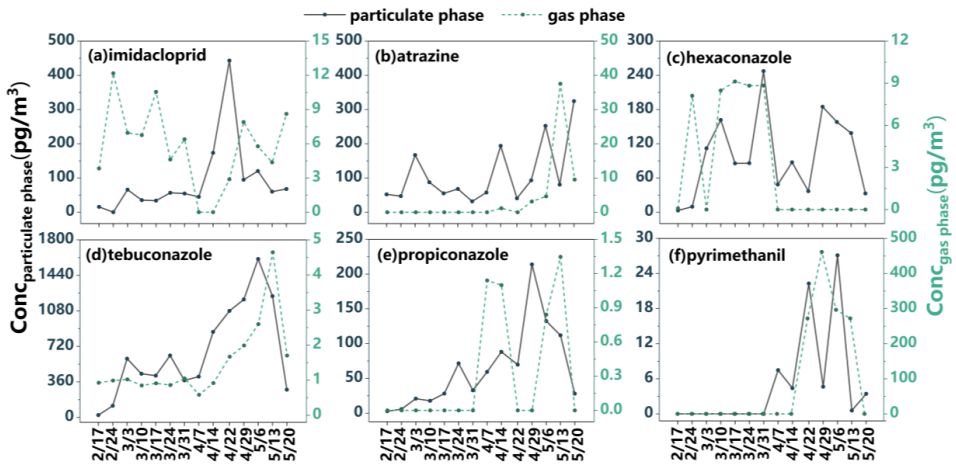


Figure 2. The concentration trend of different pesticides with sampling dates in particulate phase (full line) and gas phase (dotted line) from February 2023 to May 2023. (a) imidacloprid. (b) atrazine. (c) hexaconazole. (d) tebuconazole. (e) propiconazole. (f) pyrimethanil. The left coordinate axis represents the concentration of pesticide



324 in particulate phase and the right coordinate axis represents the concentration in gas phase.

325

326 **3.4 Effect of meteorology on pesticide concentrations in both particulate and gas phase**

327 To elucidate major factors influencing pesticide distribution between the particulate and gas
328 phases, we used a Pearson correlation matrix to visualize the relationships among total pesticide
329 concentrations in both phases, meteorological parameters, and particulate matter (PM₁₀, PM_{2.5}
330 and TSP) concentrations (Figure 3). A positive correlation with a correlation coefficient of 0.66
331 ($p < 0.01$) between the particulate and gas-phase pesticide concentrations was observed,
332 indicating that pesticides in both particulate and gas phase share common sources. A significant
333 negative correlation was observed between the pesticide concentration in particulate + gas
334 phase and reciprocal temperature ($r = -0.71$, $p < 0.01$). In other words, rising temperature leads
335 to an increase of the total concentration of pesticides in the atmosphere, including those in both
336 gaseous and particulate phases. It can be explained by that more pesticides volatilized from the
337 soil to the atmosphere with high temperature, which aligns with the finding by Iakovides et al.
338 (Iakovides et al., 2022). Figure 3 shows a lack of significant correlation between pesticide
339 concentrations (both particulate and gaseous) and wind speed, suggesting that the pesticide
340 concentration in the atmosphere in this study was dominated by local emission sources rather
341 than long-distance sources by wind. In addition, a significant negative correlation was observed
342 between reciprocal temperature and pesticide concentration in the particulate phase ($r = -0.72$,
343 $p < 0.01$), whereas no statistically significant correlation was found with the concentration in
344 the gas phase. Thus, increasing temperatures were connected to an enrichment of pesticides in
345 the particle phase. This finding is somewhat unexpected, as increased temperatures typically



promotes the phase transition of semivolatile organic compounds from the particulate to the gaseous phase. Wang et al. identified temperature as the primary factor influencing the gas-particle partitioning of polycyclic aromatic hydrocarbons (PAHs) (Wang et al., 2024). Atmospheric pesticide concentrations showed no significant correlations with precipitation, relative humidity, or wind speed. Negative correlations ($r = -0.54$ to -0.32) were observed between pesticide concentrations (in both particulate and gas phases) and levels of PM_{10} or $PM_{2.5}$.

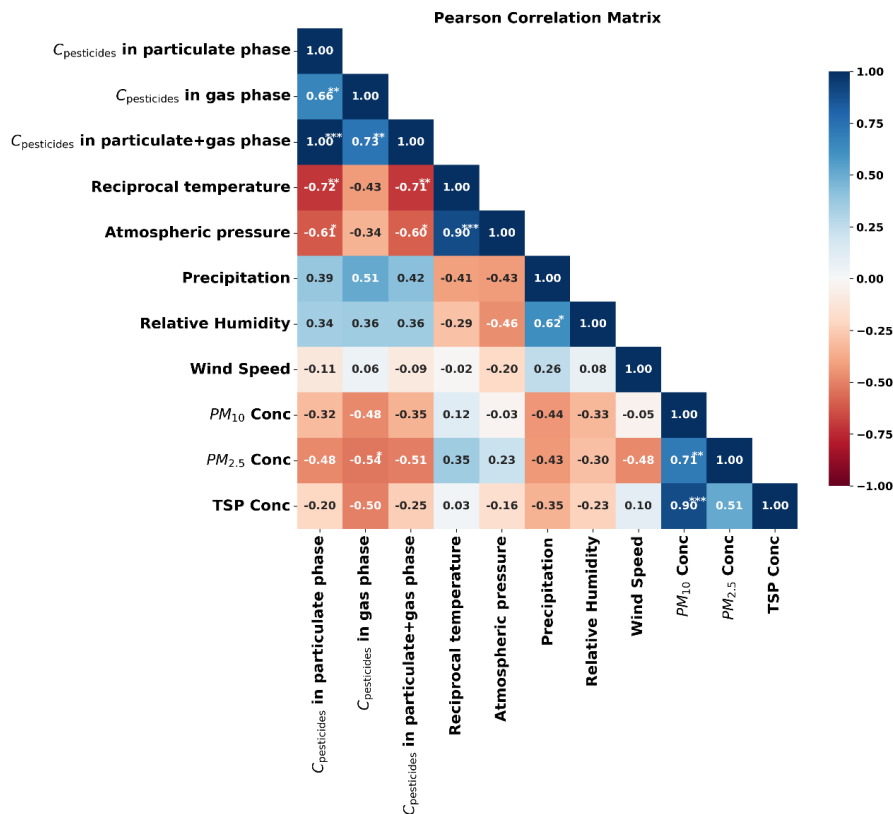


Figure 3. Pearson correlation matrix of pesticide concentrations in particulate phase, gas phases and particulate+gas phase with meteorological parameters and particulate matter (PM_{10} , $PM_{2.5}$ and TSP) concentrations. The values in

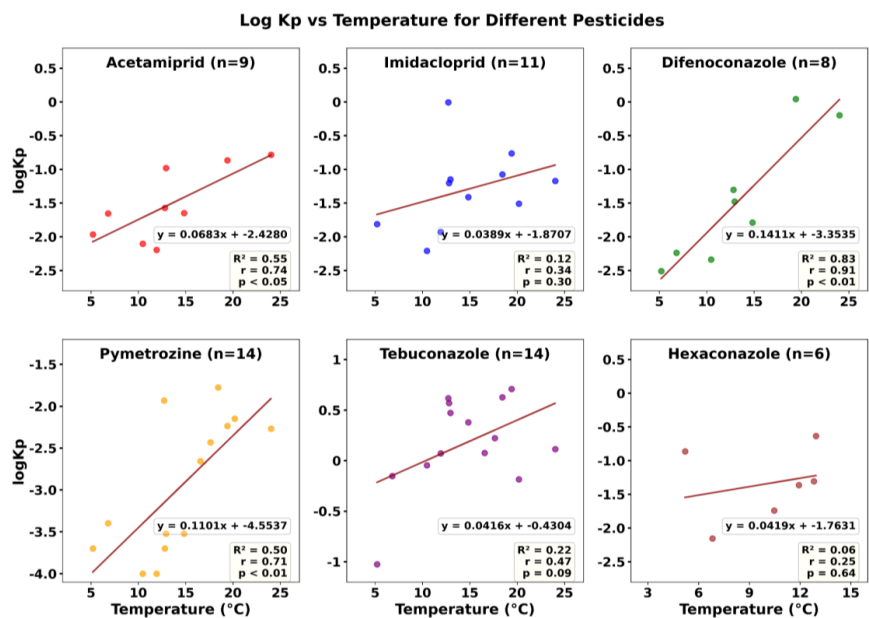


the cells represent Pearson correlation coefficients (r). Asterisks indicate statistical significance: $*p < 0.05$, $**p < 0.01$, and $***p < 0.001$.

To further investigate the influence of temperature, we performed a correlation analysis between temperature and the $\log K_p$ values of pesticides meeting the criterion of having more than five valid data points (i.e., acetamiprid, imidacloprid, difenoconazole, pymetrozine, tebuconazole, and hexaconazole), as shown in Figure 4. The $\log K_p$ values of all six pesticides increased with rising temperature. Notably, this correlation was statistically significant for acetamiprid, difenoconazole, and pymetrozine, indicating that higher temperatures were associated to their partitioning into the particulate phase. This pattern was mirrored by the relationship between temperature and the ratio of particulate-phase to gaseous-phase concentration (C_p/C_g) (Figure S4). A study by Zhu et al. in Harbin City, China reported negative correlations between temperature and $\log K_p$ for most 4–5 ring PAHs, whereas positive correlations were observed for the 3-ring PAHs (acenaphthylene and acenaphthene) (Zhu et al., 2021). This contrast highlights the pivotal role of physicochemical properties, which can lead to completely opposing temperature dependencies for $\log K_p$. Ulteriorly, the positive correlation between temperature and the particulate-phase fraction of pesticides, shown in Figure S5, may be compounded by concurrent increases in relative humidity. Specifically, when temperatures exceed 290 K, relative humidity is consistently observed to be above 52%. Under these conditions, elevated humidity can induce a phase transition in particulate matter, decreasing its viscosity and transforming it into a liquid-like state (Li and Shiraiwa, 2019). This physical change subsequently strengthens the particle's capacity to absorb and retain pesticides. Furthermore, agricultural activities (e.g., soil tillage) subsequent to pesticide application in



378 spring can accelerate the release of fine soil particles containing pesticides to the atmosphere
379 by wind erosion, resulting in the increase of pesticides in the particulate phase (Mayer et al.,
380 2024).
381



382
383 Figure 4 The correlation between log K_p for pesticides and temperature. The "n" in the figure represents the number
384 of valid data points for each type of pesticide in the logK_p measurement. Pearson correlation analysis was conducted
385 between log K_p and temperature for pesticides with more than five valid data points. R² represents the coefficient
386 of determination for Pearson correlation, r represents the correlation coefficient, and p represents the significance
387 level.

388 3.5 Gas-Particle partitioning

389 In order to investigate the distribution of pesticides in the atmosphere of Quzhou County, the



390 NCP, we analyzed the partitioning of pesticides between the gas phase and the particulate phase.

391 The gas-particle partitioning coefficient K_P calculated by equation (1) are summarized in Table

392 S9. In general, tebuconazole exhibited the highest partition coefficient (K_P , 0.09–5.1 m³/pg)

393 across all sampling periods, indicating a greater tendency for distribution in the particulate

394 phase, likely due to its low saturation vapor pressure of supercooled liquid (P_L^0). The K_P of

395 pymetrozine was markedly low from the February 17th to March 31st in 2023 and increased

396 significantly from April^{7th} to May^{20th} in 2023, indicating an approximate tenfold variation. This

397 phenomenon may be attributed to the progressive partitioning of pymetrozine into the

398 particulate phase over time. Alternatively, the increased application of pesticides during the

399 booting and heading stages of wheat could also be a contributing factor. During these stages,

400 the elevated pesticide usage may lead to emission into the atmosphere, where the pesticides

401 subsequently bind to atmospheric particulate matter. Other pesticides, including acetamiprid,

402 imidacloprid and difenoconazole, also showed the same pattern of K_P .

403 Measured particle-bound fraction ϕ of 18 pesticides detected in the gas phase and the particulate

404 phase were plotted against the corresponding P_L^0 and compared with theoretical curves at given

405 θ representing remote, rural and urban areas. Overall, the results presented in Figure 5 show

406 that most ϕ values ranged from 0.7 to 1, suggesting a potential underestimation of ϕ and

407 highlighting the limitations of the adsorptive model in accurately simulating ϕ for most

408 pesticides. This also implies the possible involvement of additional absorption mechanisms

409 beyond surface adsorption.

410 While gas-particle partitioning models mostly assume thermodynamic equilibrium, kinetic

411 effects that lead to non-equilibrium states are not captured by the models. Under field conditions,



412 several factors, such as pesticide source and transport (e.g., drift, volatilization after application
413 and wind erosion of contaminated soil), the interval between application and sampling, the
414 distance between application and sampling sites, and environmental conditions, might
415 significantly affect gas-particle partitioning (Scheyer et al., 2008). Therefore, the
416 underestimation may be due to pesticides, deposited on soil surfaces, that were resuspended
417 into the atmosphere by wind erosion, and sampled before gas-particle partitioning reached an
418 equilibrium state.

419 Furthermore, some uncertainties associated with sampling and analysis methods could also
420 contribute to differences between theoretical and experimental data. For example, about half of
421 the P_L^0 values used in predictive models were calculated at 25°C by the U.S.EPA's EPI suite
422 (v.4.1). In this study, however, samples were collected in winter and spring at temperatures
423 considerably lower than 25°C (i.e., 0.5–22°C). Considering that P_L^0 of pesticides decreases with
424 lower temperatures, partitioning into the particulate phase is favored. Consequently, there were
425 more pesticides distributing in the particulate phase under actual conditions, which caused
426 higher particle fraction (φ_m) of each pesticide and underestimation of the model. In addition,
427 due to the lack of adequate field measurements, c and θ values were estimated from other
428 studies. Since the constant c varies for different groups of compounds, the value of 17.2 Pa/cm
429 may not always be appropriate for each pesticide. The value of θ was also affected by the
430 heterogeneous composition of atmospheric aerosols (contents of organic and elemental carbon),
431 introducing uncertainty into model predictions. Additionally, the results further confirmed that
432 the surface area of particulate matter in China may differ from that in Western Europe and the
433 United States (Fleagle, 1963; Harner and Bidleman, 1998). The air pollution in China is caused



by the production of highly primary emissions and secondary aerosols, while the Great Smog
of London and Los Angeles mainly resulted from coal combustion and photochemical oxidation
of vehicle emissions, respectively (An et al., 2019). Therefore, the actual contaminated TSP
surface area per unit of air volume in Quzhou County should be greater than $1.1 \times 10^{-5} \text{ cm}^2/\text{cm}^3$,
which was used in this model for the urban area.

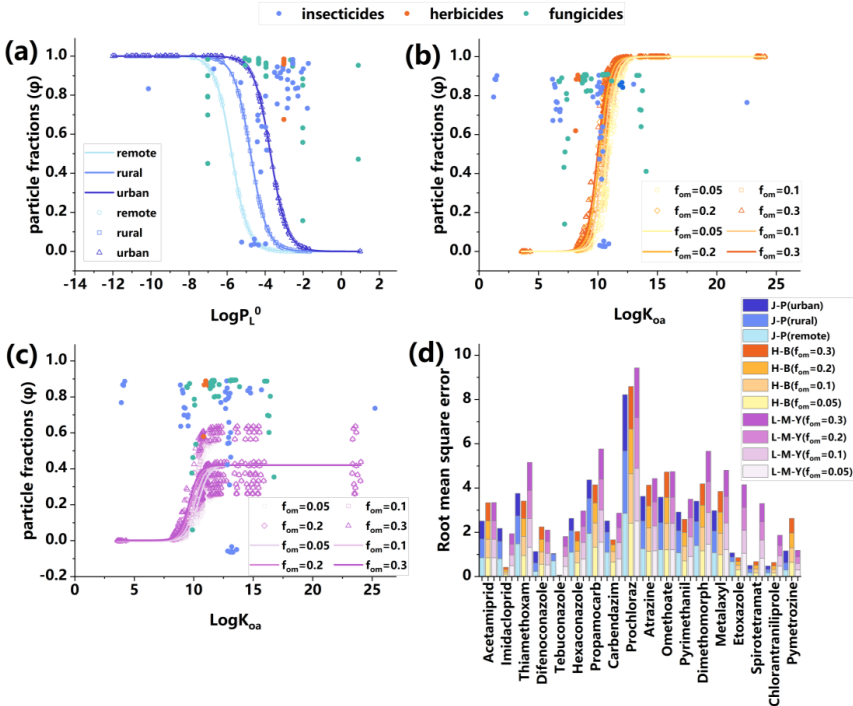


Figure 5. Measured vs. predicted particle fractions (ϕ) by applying J-P model (a), H-B model (b) and L-M-Y model (c) for 18 major pesticides detected both in particulate phase and gas phase. (d) The root mean square error (RMSE) of the particle phase fractions of 18 pesticides predicted by the J-P model, H-B model and L-M-Y model. The different colored lines represent remote, rural, and urban areas with different contaminated aerosol surface area per



444 air volume unit and different f_{om} . The different colored full dots represent different pesticides (i.e., insecticides,
 445 herbicides and fungicides), empty dots represent model prediction ϕ value.

446 In addition to the J-P adsorption model (Figure 5a), measured ϕ particle fractions for 18
 447 pesticides detected in both the particulate phase and gas phase were plotted against their
 448 corresponding $\log K_{oa}$ values and compared with theoretical partitioning curves at given f_{om}
 449 values (0.05, 0.1, 0.2 and 0.3) based on the H-B absorptive model (Iakovides et al., 2022). As
 450 shown in Figure 5b, the ϕ values predicted by the K_{oa} absorption model exhibited greater
 451 alignment with theoretical values compared to those predicted by the J-P adsorption model. The
 452 fitting of the pesticides (atrazine, prochloraz, hexaconazole and imidacloprid) with $\log K_{oa}$ in
 453 the range of 9.98–12.10 was better, with prochloraz and hexaconazole exhibiting the most
 454 precise fitting. This indicates that, compared to the adsorption mechanism, the absorption
 455 mechanism was the main mechanism to describe the gas-particle partitioning of the pesticides,
 456 This might be related to the fact that the increase in temperature causes K_{oa} to increase (Eq 4),
 457 thereby facilitating the distribution of pesticides into the organic phase, which is consistent with
 458 the previous analysis of influencing factors.

459 For pesticides with $\log K_{oa}$ values less than 9.98 (omethoate, acetamiprid, propamocarb,
 460 metalaxyl and pyrimethanil), all four prediction curves were significantly underestimated. This
 461 discrepancy can be attributed to the calculation of K_{oa} values in the model based on the K_{ow}
 462 equation at 25°C, while the samples were collected in winter and spring at temperatures lower
 463 than 25°C. Considering that the K_{oa} of pesticides increases with the decreasing temperature,
 464 this weakens the trend of the transformation into the gas phase, resulting in more pesticides
 465 distributing in the particulate phase under actual conditions, and caused higher ϕ values.



466 However, for the pesticides with LogK_{oa} bigger than 12.10 (difenoconazole, thiamethoxam,
 467 chlorantraniliprole and partial pymetrozine), there was overestimation in all of four curves,
 468 which may be related to the fact that the gas-particle partitioning of these pesticides did not
 469 reach the equilibrium state. Both K_{oa} and P_L^0 model observations described above imply that
 470 adsorptive and absorptive partitioning are not strong standalone predictors for the pesticides in
 471 the studied atmosphere.

472 Measured ϕ particle fractions for the 18 pesticides mentioned above were also plotted against
 473 their corresponding logK_{oa} values and associated with theoretical curves at given f_{om} values
 474 (0.05, 0.1, 0.2 and 0.3) based on the L-M-Y steady-state model. As shown in Figure 5c, the L-
 475 M-Y model underestimated the distribution in the particulate phase for almost all of the
 476 pesticides, and the fitting performance of the model was inferior to that of the H-B model,
 477 indicating that the distribution of pesticides on particulate matter was closer to the equilibrium
 478 state than that of the steady state. In addition, the farther the distance from the pesticide
 479 application sites to the sampling sites, the higher the proportion of pesticides that distribute in
 480 the particulate phase (Amelia et al., 2005). Therefore, in this model, the underestimation of ϕ
 481 values may stem from both local sources and long-range atmospheric transport of pesticides.

482 To better identify the prediction outputs of the three models, the RMSE for each ϕ_p of the
 483 pesticides detected in the gas phase and the particulate phase at the same time was calculated.
 484 As shown in Figure 5d, for most of the pesticides, the RMSE values of the L-M-Y model were
 485 higher than those of the other two models, indicating that the L-M-Y model had poorer
 486 predictive performance. The RMSE values of the J-P and H-B models were comparable, with
 487 the H-B model yielding lower RMSE values for 8 pesticides and the J-P model yielding lower



488 RMSE values with 10 pesticides. Although more pesticides fitted with the J-P model achieved
 489 lower RMSE values compared to the H-B model, the mean RMSE value of the H-B model was
 490 lower than that of J-P model, suggesting slightly stronger predictive capability of the H-B model
 491 for ϕ values.

492 Additionally, the trends of the logarithm of the measured gas-particulate partition coefficient
 493 (K_{pm}) to the predicted gas-particulate partition coefficient (K_{pp}) and K_{oa} log-log relationships for
 494 the H-B model and L-M-Y model were also explored and the closer the slope derived from the
 495 fitting line to 0, the better the agreement between K_{pm} and K_{pp} and the results are shown in
 496 Figure S3. Compared to the H-B model, the slope of $\text{Log}K_{pm}/\text{Log}K_{pp}$ and $\text{Log}K_{oa}$ fitting line
 497 predicted by L-M-Y model was closer to 0, indicating that the L-M-Y model may have better
 498 predictive performance. However, both of the two models produced lower R^2 , which might be
 499 due to excessive $\text{Log}K_{pm}/\text{Log}K_{pp}$ values for individual pesticides (pymetrozine, tebuconazole
 500 and imidacloprid). Therefore, this chapter considers the actual fitting performance of each
 501 model and the results calculated according to RMSE in particular.

502 In general, the K_P of tebuconazole was the highest in each sampling period, indicating that the
 503 pesticide was more likely to be distributed in particulate phase during the sampling period,
 504 likely due to its low P^0_L . The K_P values of pymetrozine, acetamiprid, imidacloprid and
 505 difenoconazole were very low in the first half of the entire sampling period and increased in the
 506 last half of the entire sampling period, owing to the fact that more pesticides distributing into
 507 the particulate phase as time went on or due to an increasing number of pesticides applied in
 508 the fields around sampling site. Compared with the other two models, the H-B model could
 509 better predict the gas-particle partitioning of pesticides in the atmosphere in Quzhou. The



510 absorption mechanism was the main mechanism to describe the partitioning on particulate
511 matter, but it was not an independent predictor, and other mechanisms were also controlling the
512 gas-particle partitioning. In addition, the gas-particle partitioning in the atmosphere was closer
513 to the equilibrium state rather than the steady state, but it still had not reached equilibrium state.

514 **4 Limitation**

515 This study has the following two limitations. To achieve sufficient analyte mass for detection
516 at low flow rates, a seven-day sampling period was employed. However, such prolonged
517 collection may result in the redistribution of pesticides between the gas and particulate phases
518 on the sampler media, potentially biasing the observed phase distribution. In addition, we
519 estimated the gas-particle partitioning coefficient (K_p) using four assumed fractions of organic
520 matter (f_{om})—5%, 10%, 20%, and 30%—rather than measured organic matter content. This
521 approach may influence predictions of pesticide adsorption to particulate phases, as adsorption
522 is often strongly correlated with organic matter content.

523 **5 Conclusions**

524 Utilizing UHPLC-MS/MS method and partitioning prediction models, this study focused on
525 the gas-particle partitioning of pesticides in Quzhou County, the NCP. Our study demonstrates
526 that pesticides were predominantly present in the particulate phase, accounting for up to 93.4 %
527 of the total concentration in the atmosphere. The concentrations of most pesticides in the
528 particulate phase and gas phase reach the maximum between mid-April and May suggesting
529 that regional pesticide application patterns drive the temporal concentration trends. It was found
530 that an increase in temperature significantly promoted the concentration of pesticides in the
531 atmosphere. Moreover, a positive correlation between temperature and particulate-phase



pesticide concentrations was observed, as indicated by rising $\log K_p$ values. This pattern is likely driven by a combination of factors, including pesticide physicochemical properties, ambient relative humidity, particle phase state and pesticide use patterns. The H-B model could better predict the gas-particle partitioning of pesticides in the atmosphere, and the absorption mechanism is the main mechanism to describe the partitioning on particulate matter. In general, this study indicates that pesticides are mainly absorbed into the internal organic films of particulate matter in the NCP and advances the understanding of pesticide fate in the atmosphere of the NCP. To further elucidate pesticide behavior in particulate matter, future study should investigate the occurrence and transformation of pesticides across different particle size fractions, especially the fine particles.

542

543 **Data Availability**

The data sets generated in the current study are available at https://zenodo.org/records/17641894?preview=1&token=eyJhbGciOiJIUzUxMiJ9.eyJpZCI6ImM0ZDAwOWUwLTU4YjAtNGFmMy1iZGFjLWE4YWVjZmE4NDE1ZSIsImRhdGEiOiOnt9LCJyYW5kb20iOiI2ZDhhMTU4MDc1Zjg4YThjODFiZTk5Zjk0ZTI5OTE2NyJ9.R1A8yqr2bWZgp_fe95aDW33pY5MJof8vFbG8tap-dAiQk9jQJOU_fHWipa8of7cdn0GzqRHyy2-USZeDjk-5VQ (Guo et al., 2025, <https://doi.org/10.5281/zenodo.17641894>). Figures were made with Matplotlib version 3.8.4 (<https://zenodo.org/records/10916799>), available under the Matplotlib license at <https://matplotlib.org/>.



553 **Supporting Information**

554 The detailed description of calculation of the mass concentration of pesticides in ambient air
 555 (text S1); the trend of different pesticide concentrations in particulate phase with time during
 556 the sampling period from February 2023 to May 2023 (Figure S1); the trend of different
 557 pesticide concentrations in gas phase with time during the sampling period from February 2023
 558 to May 2023 (Figure S2); the slope of $\text{LogK}_{\text{pm}}/\text{LogK}_{\text{pp}}$ and LogK_{oa} fitting line predicted by L-
 559 M-Y model and H-B model (Figure S3); the correlation between C_g/C_p for pesticides and
 560 temperature (Figure S4); the correlation between particulate-phase pesticide concentration and
 561 temperature (Figure S5); the information of the samples (Table S1); the information of the
 562 meteorological data in the sampling period (Table S2); the information of standard substance
 563 (Table S3); the limit of quantitation and limit of detection (Table S4); the $\log P_L^0$ of each
 564 pesticide in each sampling period (Table S5); the $\log K_{\text{oa}}$ of each pesticide in each sampling
 565 period (Table S6); the detection frequency of the pesticides in gas phase and particulate phase
 566 (Table S7); the concentration of the pesticides in gas phase and particulate phase (Table S8);
 567 the gas-particle partition coefficients of the pesticides (Table S9).

568

569 **Author contributions**

570 Kai Wang contributed in designed the experiments and fundings for this work. Liping Guo was
 571 responsible for data analysis and manuscript preparation. Shuping Shi is responsible for
 572 conducting the experiment. Mingyu Zhao and Hongyu Mu provided guidance for the



573 experiment. Ying Li provided guidance on the gas-particle partitioning model part. Martin Brü
574 ggemann, Daniel M. Figueiredo and Junxue Wu provided guidance on article writing.

575

576 **Competing interests**

577 The authors declare that they have no known competing financial interests or personal
578 relationships that could have appeared to influence the work reported in this paper.

579 **Acknowledgements**

580 The authors gratefully acknowledge the financial support from the National Natural Science
581 Foundation of China (No. 42207125 and No. 42475124); Professor Station of China
582 Agricultural University at Xinzhou Center for Disease Control and Prevention; Mingyu Zhao
583 acknowledges the China Scholarship Council (No. 201913043).

584 **Financial support**

585 This research has been supported by the National Natural Science Foundation of China (No.
586 42207125 and No. 42475124), Professor Station of China Agricultural University at Xinzhou
587 Center for Disease Control and Prevention and the China Scholarship Council (No. 201913043).

588



References

- Aktar, M. W., D. Sengupta, and A.: Chowdhury. Impact of pesticides use in agriculture: their benefits and hazards, *Interdisciplinary toxicology*, 2(1), 1, <http://doi.org/10.2478/v10102-009-0001-7>, 2009.
- Amelia, S, Clymo, Jin, Young, Shin, Britt, A, and Holmén.: Herbicide Sorption to Fine Particulate Matter Suspended Downwind of Agricultural Operations: Field and Laboratory Investigations, *Environ. Sci. Technol.*, 39(2), 421–430, <http://doi.org/10.1021/es049210s>, 2005.
- An, Z., R. J. Huang, R. Zhang, X. Tie, G. Li, J. Cao, W. Zhou, Z. Shi, Y. Han, and Z. Gu.: Severe haze in northern China: A synergy of anthropogenic emissions and atmospheric processes, *Proceedings of the National Academy of Sciences of the United States of America*, 116(18), 8657-8666, <http://doi.org/10.1073/pnas.1900125116>, 2019.
- Baskaran, S., Y. D. Lei, and F. Wania.: Reliable Prediction of the Octanol-Air Partition Ratio, *Environ Toxicol Chem*, 40(11), 3166-3180, <http://doi.org/10.1002/etc.5201>, 2021.
- Bedos, C., P. Cellier, R. Calvet, and E. Barriuso.: Occurrence of pesticides in the atmosphere in France, *Agronomie*, 22(1), 35-49, <http://doi.org/10.1051/agro:2001004>, 2002.
- Brüggemann, M., S. Mayer, D. Brown, A. Terry, J. Rüdiger, and T. Hoffmann.: Measuring pesticides in the atmosphere: current status, emerging trends and future perspectives, *Environmental Sciences Europe*, 36(1), 39, <http://doi.org/10.1186/s12302-024-00870-4>, 2024.
- Cabrerizo, A., J. Dachs, K. C. Jones, and D. Barceló.: Soil-Air exchange controls on background atmospheric concentrations of organochlorine pesticides, *Atmos. Chem. Phys.*, 11(24), 12799-12811, <http://doi.org/10.5194/acp-11-12799-2011>, 2011.
- Ministry of Agriculture and Rural Affairs of the People's Republic of China.: The goal of achieving zero growth in the usage of fertilizers and pesticides has been successfully accomplished. https://www.moa.gov.cn/xw/zwdt/202101/t20210117_6360031.htm, 2021.
- Cui, J. K., Huang, W. K., Peng, H. Lv, Y., Kong, L. A., Li, H. X., Luo, S.-J., Wang, Y. and Peng, D. L.: Efficacy Evaluation of Seed-Coating Compounds Against Cereal Cyst Nematodes and Root Lesion Nematodes on Wheat, *Plant Disease*, 101(3), 428-433, <http://doi.org/10.1094/PDIS-06-16-0862-RE>, 2016.
- Degrendele, C., K. Okonski, L. Melymuk, L. Landlova, P. Kukucka, O. Audy, J. Kohoutek, P. Cupr, and J. Klanova.: Pesticides in the atmosphere: a comparison of gas-particle partitioning and particle size distribution of legacy and current-use pesticides, *Atmos. Chem. Phys.*, 16(3), 1531-1544, <http://doi.org/10.5194/acp-16-1531-2016>, 2016.
- FAO.: Pesticides use and trade – 1990–2023. FAOSTAT Analytical Briefs, No. 109. Rome. , <http://doi.org/https://doi.org/10.4060/cd5968en>, 2025.
- Feng, S. J., Xu, W., Cheng, M. M., Ma, Y. X., Wu, L. B., Kang, J. H., Wang, K., Tang, A. H., Jeffrey L. C J., Fang, Y. T., Keith, G., Liu, X. J., Zhang F. S.: Overlooked Nonagricultural and Wintertime Agricultural NH₃ Emissions in Quzhou County, North China Plain: Evidence from ¹⁵N-Stable Isotopes, *Environ. Sci. Tech. Let.*, 9(2), 127-133, <http://doi.org/10.1021/acs.estlett.1c00935>, 2022.
- Fleagle, R. G.: Atmospheric processes, *Science*, 140(3567), 653-654, <http://doi.org/10.1126/science.140.3567.653.b>, 1963.
- Glotfelty, D. E., M. M. Leech, J. Jersey, and A. W. Taylor: Volatilization and wind erosion of soil surface applied atrazine, simazine, alachlor, and toxaphene, *Journal of agricultural and food chemistry*, 37(2), 546-551, <http://doi.org/10.1021/jf00086a059>, 1989.
- Gungormus, E., A. Sofuoglu, H. Celik, K. Gedik, M. D. Mulder, G. Lammel, S. C. Sofuoglu, E. Okten, T. Ugranlı, and A. Birgül.: Selected persistent organic pollutants in ambient air in Turkey: Regional



sources and controlling factors, *Environ. Sci. Technol.*, 55(14), 9434-9443, <http://doi.org/10.1021/acs.est.0c06272>, 2021.

Guo, L. P., Shi, S. P., Li, Y., M. Brüggemann, Zhao, M. Y., Mu, H. Y., D. M. Figueiredo, Wu, J. X. and Wang, K.: Gas-particle partitioning of pesticides in the atmosphere of the North China Plain [Dataset], Zenodo, <https://doi.org/10.5281/zenodo.17641894>, 2025.

Harner, T., and T. F. Bidleman.: Octanol– air partition coefficient for describing particle/gas partitioning of aromatic compounds in urban air, *Environ. Sci. Technol.*, 32(10), 1494-1502, [http://doi.org/10.1016/S1352-2310\(97\)00013-7](http://doi.org/10.1016/S1352-2310(97)00013-7), 1998.

He, J. and R.: Balasubramanian. A study of gas/particle partitioning of SVOCs in the tropical atmosphere of Southeast Asia, *Atmos. Environ.*, 43(29), 4375-4383, <http://doi.org/10.1016/j.atmosenv.2009.03.055>, 2009.

Hu, Y., Wu, S., Wu, C., Wei, Z., Ning, J. and D. She.: Risk assessment of airborne agricultural pesticide exposure in humans in rural China, *Environ Geochem Health*, 46(4), 117, <http://doi.org/10.1007/s10653-024-01882-y>, 2024.

Iakovides, M., K. Oikonomou, J. Sciare, and N. Mihalopoulos.: Evidence of stockpile contamination for legacy polychlorinated biphenyls and organochlorine pesticides in the urban environment of Cyprus (Eastern Mediterranean): influence of meteorology on air level variability and gas/particle partitioning based on equilibrium and steady-state models, *J. Hazard. Mater.*, 439, 129544, <http://doi.org/10.1016/j.jhazmat.2022.129544>, 2022.

Jiang, L., Gao, W., Ma, X., Wang, Y., Wang, C., Li, Y., Yang, R., Fu, J., Shi, J., Zhang, Q. H., Wang, Y. W., Jiang, G. B.: Long-term investigation of the temporal trends and gas/particle partitioning of short- and medium-chain chlorinated paraffins in ambient air of King George Island, Antarctica, *Environ. Sci. Technol.*, 55(1), 230-239, <http://doi.org/10.1021/acs.est.0c05964>, 2020.

Kaur, R., G. K. Mavi, S. Raghav, and I. Khan.: Pesticides classification and its impact on environment, *Int. J. Curr. Microbiol. Appl. Sci.*, 8(3), 1889-1897, <http://doi.org/10.20546/ijcmas.2019.803.224>, 2019.

Li, Y., and M. Shiraiwa.: Timescales of secondary organic aerosols to reach equilibrium at various temperatures and relative humidities, *Atmos. Chem. Phys.*, 19(9), 5959-5971, <http://doi.org/10.5194/acp-19-5959-2019>, 2019.

Lohmann, R., F. M. Jaward, L. Durham, J. L. Barber, W. Ockenden, K. C. Jones, R. Bruhn, S. Lakaschus, J. Dachs, and K. Booij.: Potential contamination of shipboard air samples by diffusive emissions of PCBs and other organic pollutants: Implications and solutions, *Environ. Sci. Technol.*, 38(14), 3965-3970, <http://doi.org/10.1021/es035005l>, 2004.

Mayer, L., C. Degrendele, P. Šenk, J. Kohoutek, P. Přibyllová, P. Kukučka, L. Melymuk, A. Durand, S. Ravier, A. Alastuey, A. R. Baker, U. Baltensperger, K. Baumann-Stanzer, T. Biermann, P. Bohlin-Nizzetto, D. Ceburnis, S. Conil, C. Couret, A. Degórska, E. Diapouli, S. Eckhardt, K. Eleftheriadis, G. L. Forster, K. Freier, F. Gheusi, M. I. Gini, H. Hellén, S. Henne, H. Herrmann, A. Holubová Šmejkalová, U. Hörrak, C. Hüglin, H. Junninen, A. Kristensson, L. Langrene, J. Levula, M. Lathon, E. Ludewig, U. Makkonen, J. Matejovičová, N. Mihalopoulos, V. Mináriková, W. Moche, S. M. Noe, N. Pérez, T. Petäjä, V. Pont, L. Poulain, E. Quivet, G. Ratz, T. Rehm, S. Reimann, I. Simmons, J. E. Sonke, M. Sorribas, R. Spoor, D. P. J. Swart, V. Vasilatou, H. Wortham, M. Yela, P. Zarmpas, C. Zellweger Fäsi, K. Tørseth, P. Laj, J. Klánová, and G. Lammel.: Widespread Pesticide Distribution in the European Atmosphere Questions their Degradability in Air, *Environ. Sci. Technol.*, 58(7), 3342-3352, <http://doi.org/10.1021/acs.est.3c08488>, 2024.



- 677 McEachran Andrew, D., R. Blackwell Brett, J. D. Hanson, J. Wooten Kimberly, D. Mayer Gregory, B.
678 Cox Stephen, and N. Smith Philip.: Antibiotics, Bacteria, and Antibiotic Resistance Genes: Aerial
679 Transport from Cattle Feed Yards via Particulate Matter, *Environ. Health Perspect.*, 123(4), 337-343,
680 <http://doi.org/10.1289/ehp.1408555>, 2015.
- 681 Ministry of Agriculture and Rural Affairs of the People's Republic of China.: Ministry of Agriculture,
682 Ministry of Industry and Information Technology, Ministry of Environmental Protection
683 Announcement No. 1157, edited,
684 http://www.moa.gov.cn/nybg/2009/dsanq/201806/t20180606_6151221.htm, 2009.
- 685 Ngo, M., K. Pinkerton, S. Freeland, M. Geller, W. Ham, S. Cliff, L. Hopkins, M. Kleeman, U. Kodavanti,
686 and E. Meharg.: Airborne particles in the San Joaquin Valley may affect human health, *California*
687 *Agriculture*, 64(1), 12-16, <http://doi.org/10.3733/ca.v064n01p12>, 2010.
- 688 Pankow, J. F.: Review and comparative analysis of the theories on partitioning between the gas and
689 aerosol particulate phases in the atmosphere, *Atmospheric Environment* (1967), 21(11), 2275-2283,
690 [http://doi.org/10.1016/0004-6981\(87\)90363-5](http://doi.org/10.1016/0004-6981(87)90363-5), 1987.
- 691 Qiao, L. N., Zhang, Z. F., Liu, L. Y., Song, W. W., Ma, W. L., Zhu, N. Z. and Li, Y. F.: Measurement and
692 modeling the gas/particle partitioning of organochlorine pesticides (OCPs) in atmosphere at low
693 temperatures, *Sci. Total Environ.*, 667, 318-324, <http://doi.org/10.1016/j.scitotenv.2019.02.347>, 2019.
- 694 Sanli, G. E., and Y. Tasdemir.: Seasonal variations of organochlorine pesticides (OCPs) in air samples
695 during day and night periods in Bursa, Turkey, *Atmospheric Pollution Research*, 11(12), 2142-2153,
696 <http://doi.org/10.1016/j.apr.2020.06.010>, 2020.
- 697 Scheyer, A., S. Morville, P. Mirabel, and M. Millet.: Gas/particle partitioning of lindane and current-used
698 pesticides and their relationship with temperature in urban and rural air in Alsace region (east of
699 France), *Atmos. Environ.*, 42(33), 7695-7705, <http://doi.org/10.1016/j.atmosenv.2008.05.029>, 2008.
- 700 Socorro, J., A. Durand, B. Temime-Roussel, S. Gligorovski, H. Wortham, and E. Quivet.: The persistence
701 of pesticides in atmospheric particulate phase: An emerging air quality issue, *Sci. Rep.*, 6(1), 33456,
702 <http://doi.org/10.1038/srep33456>, 2016.
- 703 Tudi, M., Li, H. R., Li, H. Y., Wang, L., Lyu, J., Yang, L. S., Tong, S. M., Q. J. Yu, H. D. Ruan, and A.
704 Atabila, D. T. Phung, R. Sadler, and D. Connell.: Exposure routes and health risks associated with
705 pesticide application, *Toxics*, 10(6), 335, <http://doi.org/10.3390/toxics10060335>, 2022.
- 706 Turusov, V., V. Rakitsky, and L. Tomatis.: Dichlorodiphenyltrichloroethane (DDT): ubiquity, persistence,
707 and risks, *Environ. Health Perspect.*, 110(2), 125-128, <http://doi.org/10.1289/ehp.02110125>, 2002.
- 708 Van den Berg, F., R. Kubiak, W. G. Benjey, M. S. Majewski, S. R. Yates, G. L. Reeves, J. H. Smelt, and
709 A. M. A. van der Linden.: Emission of Pesticides into the Air, Water, Air, and Soil Pollution, 115(1),
710 195-218, <http://doi.org/10.1023/A:1005234329622>, 1999.
- 711 Wang, D. Q., Jia, S. M., Yang, P. F., Zhu, F. J. and Ma, W. L.: Size-resolved gas-particle partitioning of
712 polycyclic aromatic hydrocarbons in a large temperature range of 50°C, *J. Hazard. Mater.*, 479,
713 135607, <http://doi.org/https://doi.org/10.1016/j.jhazmat.2024.135607>, 2024.
- 714 Wang, S. R., A. Salamova, and M. Venier.: Occurrence, Spatial, and Seasonal Variations, and Gas-
715 Particle Partitioning of Atmospheric Current-Use Pesticides (CUPs) in the Great Lakes Basin,
716 *Environ. Sci. Technol.*, 55(6), 3539-3548, <http://doi.org/10.1021/acs.est.0c06470>, 2021.
- 717 Woodrow, J. E., K. A. Gibson, and J. N. Seiber.: Pesticides and related toxicants in the atmosphere,
718 *Reviews of Environmental Contamination and Toxicology*, 247, 147-196,
719 http://doi.org/10.1007/398_2018_19, 2019.
- 720 Yu, B. G., Liu, Y.-M., Chen, X.-X., Cao, W.-Q., Ding, T. B. and Zou, C. Q.: Foliar Zinc Application to



721 Wheat May Lessen the Zinc Deficiency Burden in Rural Quzhou, China, *Frontiers in Nutrition*, 8,
 722 <http://doi.org/10.3389/fnut.2021.697817>, 2021.

723 Yúsà, V., C. Coscollà, W. Mellouki, A. Pastor, and M. De La Guardia.: Sampling and analysis of
 724 pesticides in ambient air, *Journal of Chromatography A*, 1216(15), 2972-2983,
 725 <http://doi.org/10.1016/j.chroma.2009.02.019>, 2009.

726 Zhao, M., Wu, J., D. M. Figueiredo, Zhang, Y., Zou, Z. Y., Cao, Y. X., Li, J. J., Chen, X., Shi, S. P., Wei,
 727 Z. Y., Li, J. D., Zhang, H. Y., Zhao, E. C., V. Geissen, C. J. Ritsema, Liu, X. J., Han, J. J. and Wang,
 728 K.: Spatial-temporal distribution and potential risk of pesticides in ambient air in the North China
 729 Plain, *Environ. Int.*, 182, 108342, <http://doi.org/10.1016/j.envint.2023.108342>, 2023.

730 Zhou, Y., Guo, J. Y., Wang, Z. K., Zhang, B. Y., Sun, Z., Yun, X. and Zhang, J. B.: Levels and inhalation
 731 health risk of neonicotinoid insecticides in fine particulate matter (PM_{2.5}) in urban and rural areas
 732 of China, *Environ. Int.*, 142, 105822, <http://doi.org/10.1016/j.envint.2020.105822>, 2020.

733 Zhu, F. J., Ma, W.-L., Liu, L. Y., Zhang, Z. F., Song, W. W., Hu, P. T., Li, W. L., Qiao, L. N. and Fan, H.
 734 Z.: Temporal trends of atmospheric PAHs: Implications for the gas-particle partition, *Atmos. Environ.*,
 735 261, 118595, <http://doi.org/https://doi.org/10.1016/j.atmosenv.2021.118595>, 2021.

736
 737